LITERATURE CITED

1. V. G. Babskii, N. D. Kopachevskii, A. D. Myshkis, L. A. Slobozhanin, and A. D. Tyuptsov, The Fluid Mechanics of Weightlessness [in Russian], Nauka, Moscow (1976).
2. Ngo Zui Kan, "Rotational motion of a rigid body with a cavity filled with a viscous liquid," Zh. Vychisl. Mat. Mat. Fiz., 11, No. 6 (1971).
3. W. H. Reid, "The oscillations of a viscous liquid globe with a core," Proc. London Math. Soc., 9, No. 35 (1959).
4. W. H. Reid, "The oscillations of a viscous liquid drop," Q. Appl. Math., 18, No. 1 (1960).
5. N. D. Kopachevskii and A. D. Myshkis, "Free oscillations of a liquid self-gravitating sphere with allowance for viscous and capillary forces," Zh. Vychisl. Mat. Mat. Fiz., 8, No. 6 (1968).

EXPERIMENTAL INVESTIGATION OF FLOW IN SHALLOW AND DEEP CAVITIES

V. Ya. Bogatyrev and V. A. Mukhin

UDC 532.556.2;532.574

In the article we present the results of an experimental investigation of the flow of an incompressible liquid in shallow and deep cavities of rectangular cross section using a laser Doppler velocity meter (LDVM). The tests were made in the laminar mode of flow in the channel ahead of the cavity. The distribution of the longitudinal and transverse velocity components in the central cross section of the cavity is obtained.

There are extremely few experimental data on the investigation of flow structure in cavities. The investigations have been confined mainly to visual observations [1]. Reports in which the static pressure and the shear stress at the cavity walls were measured are well known. The profiles of velocity and shear stress at the bottom of a shallow cavity (when the ratio of the length of the cavity to its depth is $L/H > 1.75$) were measured in [2]. It is impossible to build up a detailed concept of the character of the flow in cavities of different configurations on the basis of the available reports.

A detailed description of the experimental setup and the measurement procedure is given in [3]. Here we only provide certain information about the test section. The test cavities had the following dimensions: shallow — L = 40 mm, H = 20 mm; deep — L = 20 mm, H = 40 mm. The width of a cavity equaled the width of the plane section (100 mm). The cavities were located at a distance of 1500 mm from the plane section. During the measurements the focal region lay in a plane located at equal distances from the side walls of the cavity. The size of the focal region was 100 × 100 × 800 μm. The thickness of the optical glasses was 10 mm. At a distance of 60 mm from the focal region the diameter of the laser beam was 0.5-0.6 mm. The minimum distance from the walls at which the alternate measurements of the longitudinal and transverse velocity components were made is ~1 mm. Since the optical scheme of the LDVM did not permit a determination of the direction of the velocity, flow in the cavities was investigated in detail in the case when the laminar mode of liquid motion was established in the channel and cavity. In the turbulent mode of flow we investigated only the mixing zone [the region adjacent to the upper cut of the cavity can be considered as the zone of mixing of the jet formed after separation of the stream at the point x = 0, y = 0 from the stream in the cavity (Fig. 1b)] and the boundary jet propagating along the back wall of the cavity, where the direction of motion is known.

In the case of laminar flow of liquid in the channel at $Re = 1.5 \cdot 10^3$, flow with one vortex in the upper part and a stagnant zone in the lower half was observed in the cavity with L/H = 0.5. After a certain time flow with two vortices rotating in opposite directions was established. The flow patterns replaced one another. With an increase in the Reynolds

Novosibirsk. Translated from Zhurnal Prikladnoi Mekhaniki i Tekhnicheskoi Fiziki, No. 3, pp. 70-74, May-June, 1984. Original article submitted April 13, 1983.

 0021-8944/84/2503-0396$08.50 © 1984 Plenum Publishing Corporation

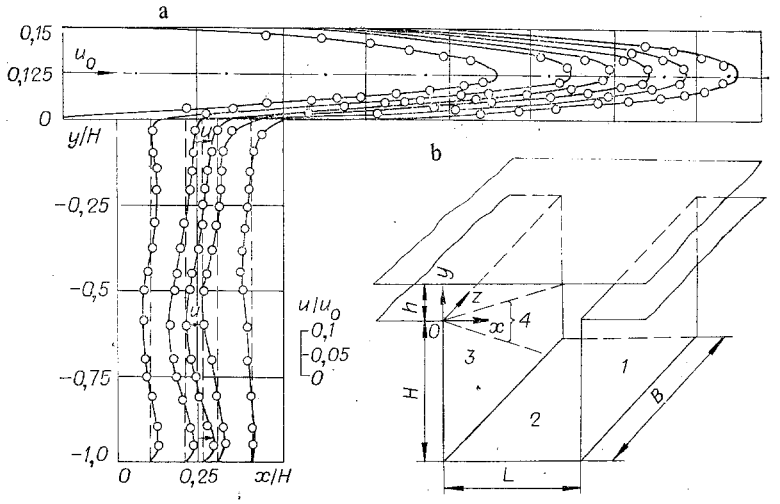

Fig. 1

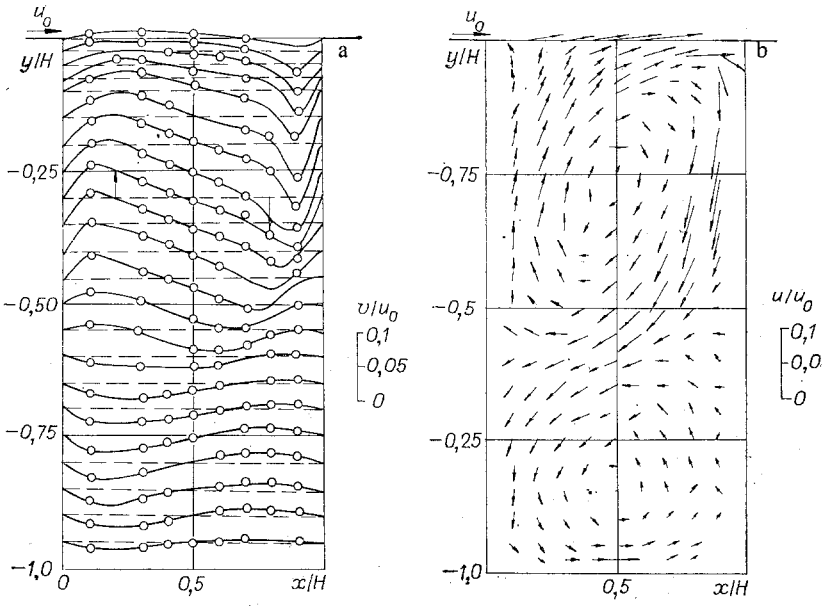

Fig. 2

number the flow with two vortices became ever more stable, and steady two-vortex motion of the liquid could be obtained at Re = $4 \cdot 10^3$. The Reynolds number was calculated from the formula Re = $u_0 2h/\nu$, where u_0 is the liquid velocity at the channel axis in the cross section located at a distance of 10 mm upstream from the cavity; h is the channel height [Fig. 1b; 1) back wall; 2) bottom; 3) front wall; 4) mixing region]. The distributions of the longitudinal and transverse velocity components, normalized to the velocity at the channel axis in the cross section x/H = −0.25, are presented in Figs. 1a and 2a while the velocity field in the entire test region, constructed from the data of Figs. 1a and 2a, is presented in Fig. 2b. It is seen that two vortices rotating in opposite directions exist in the middle cross section of the cavity. Along the upper part of the back wall a boundary jet propagates downward, which then changes direction and at the front wall separates into two parts: One part moves upward along the front wall and the other moves down along the front wall. In Figs. 1a and 2a and b it is seen that the flow in a deep cavity has a clearly three-dimensional character, since in the horizontal cross sections the liquid flow rates in the descending and ascending streams are unequal. Thus, for the horizontal cross section y/H = −0.25 passing through the center of the upper vortex the ratio of the liquid flow rate in the descending stream to the flow rate in the ascending stream is $\beta = G_1/G_2 = 1.6$. In the horizontal cross section y/H = −0.85 passing through the center of the lower vortex $\beta = 1.5$. The vortex in the upper part of the cavity has an elliptical shape with a ratio of axis lengths of 2:1. The major axis of the

ellipse is located at an angle of ~30° to the vertical axis of the cavity. Since the velocity vectors tangent to the streamlines have the same magnitudes, while the streamlines are not circles, it can be concluded that the vorticity in a cavity of this geometry is not constant.

The lower vortex has an elliptical shape with a ratio of axis lengths of 4:3. The vorticity in it is also variable. We should mention the complexities which arise in an experimental study of the velocity distribution in vortex flows and especially in the central parts of vortices. As the center of a vortex is approached, the magnitude of the velocity decreases, the relative oscillations of velocity increase, and the measurement errors grow correspondingly. Therefore, the flow pattern in the central parts of the vortices is still not clear. In [5] it was shown that in "plane" vortex flow in a cavity of square cross section a three-dimensional cellular structure develops, complicated by the presence of secondary flows in the end regions and Taylor–Gertler vortices developing along the walls of the cavity. Vortex formations vary their configurations and positions in space somewhat with time. Naturally, in a deep cavity, where two vortices interact, the picture is still more complicated. The very considerable lack of agreement of the flow rates in the ascending and descending flows (in each of the vortices) speaks in favor of this. The results obtained in the present work essentially indicate the necessity of three-component measurements of the velocity in "plane" vortex flows over the entire volume of the cavity. Profiles of the longitudinal component of the average velocity in the region adjacent to the z0x plane (see Fig. 1b) for several cross sections of the jet are presented in Fig. 3 in the coordinates $\bar{u}$ and $\eta_{1/2}$, where $\bar{u} = (u - u_2)/(u_1 - u_2)$; u_1 is the velocity at the jet axis ($\bar{y} = 0.125$); u_2 is the velocity at the outer boundary of the jet; $\eta_{1/2} = y/\delta_{1/2}$; $\delta_{1/2}$ is the conventional thickness of the jet (the distance from the jet axis where $\bar{u} = 1$ to the point at which $\bar{u} = 0.5$). Points 1-3 correspond to $\bar{x} = x/H = 0.2$, 0.3, and 0.4. The point at which $\partial u/\partial y = (\partial u/\partial y)_{core-const}$ is taken as the outer boundary of the jet. Here we also plot (solid line) the universal velocity profile in accordance with the formula [4]

$$(u - u_2)/(u_1 - u_2) = 1 - 6\eta^2 + 8\eta^3 - 3\eta^4, \quad (1)$$

where $\eta = y/\delta$; δ is is the half-width of the jet. The experimental velocity profiles in the jet practically coincide with the universal velocity profile. The velocity profile in the mixing zone in this cavity has the same character of variation along x as for $Re = 1.5 \cdot 10^3$ in a square cavity [3].

The velocity distribution at the limit of the boundary layer along the cavity walls is shown in Fig. 4. We assume that the liquid boundary layer extends from the cavity wall to the point at which the velocity has a maximum. We construct the velocity distribution at the limit of the boundary layer along the longitudinal coordinate, conditionally opening up the cavity walls into a plane (see Fig. 4). Having this dependence, we can calculate the values of the Pol'gauzen form parameter Λ, characterizing the influence of the longitudinal velocity gradient on the laminar boundary layer through the formula $\Lambda = (\delta^2/\nu)\partial u_m/\partial x$, where δ is the thickness of the boundary layer; ν is the kinematic viscosity coefficient.

The experimental profiles of the longitudinal component of the average velocity in the boundary layer in the upper part of the back wall are shown in Fig. 5a [1) $\bar{x} = 0.35$; 2) $\bar{x} = 0.45$; 3) $\bar{x} = 0.5$; 4) $\bar{x} = 0.55$; 5) $\Lambda = 0$; 6) $\Lambda = -12$].

Separation of the boundary layer, as in laminar flow in a square cavity [3], occurs at values of the form parameter Λ far exceeding the separation value of Λ ($\Lambda_{sep} = -12$). The separation velocity profile at the back wall ($\bar{x} = 0.55$) also differs considerably from the separation profile at a flat plate.

The longitudinal and transverse velocity components in a cavity with a ratio of sides L/H = 2 (L = 40 mm, H = 20 mm) are shown in Fig. 6a and b while the velocity field in a shallow cavity is shown in Fig. 6c for $Re = 1.5 \cdot 10^3$.

In such a cavity one main vortex forms, the central part of which has an approximately elliptical shape with a ratio of axis lengths of ~2:1. The major axis of the vortex is arranged horizontally and the center of the vortex has the coordinates $\bar{x} = 1.4$, $\bar{y} = -0.4$. The vorticity is not constant in it. A secondary vortex rotating in the opposite direction forms in the lower left-hand corner of the cavity. The area occupied by the secondary vortex is 20% of the cross-sectional area of the cavity.

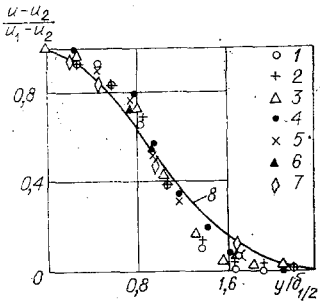

Fig. 3

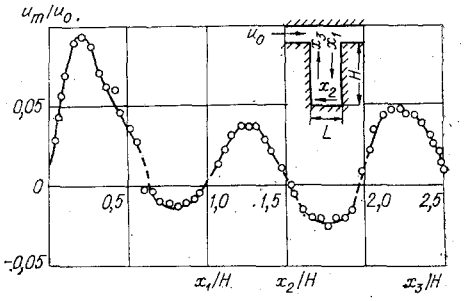

Fig. 4

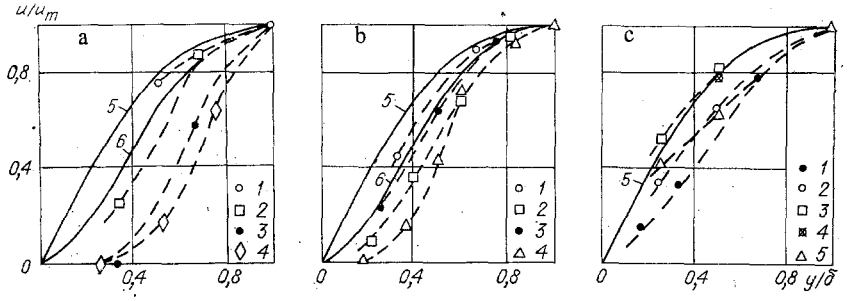

Fig. 5

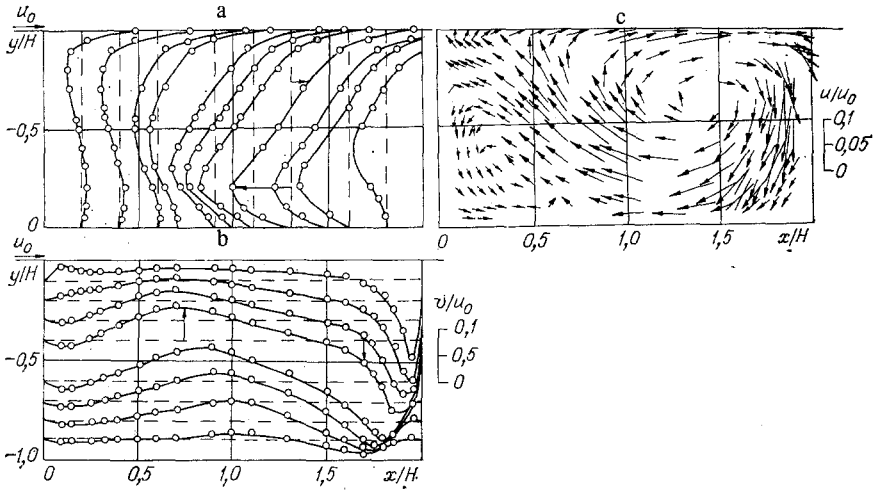

Fig. 6

It follows from Fig. 6 that removal of liquid from the cavity is observed over most of the upper cross section of the cavity (along the line $\bar{y} = 0$), and only at $\bar{x} = 1.7$ does the flow turn into the cavity. The ratio of the flow rates of the descending and ascending streams is $\beta = 0.825$ at $\bar{y} = -0.2$ and $\beta = 0.9$ at $\bar{y} = -0.5$.

The velocity profiles in the boundary layer at the back wall and bottom of the cavity in the region of the main vortex are shown in Fig. 5 [b) back wall; 1) $\bar{x} = 0.25$; 2) $\bar{x} = 0.3$; 3) $\bar{x} = 0.35$; 4) $\bar{x} = 0.4$; 5) $\Lambda = 0$; 6) $\Lambda = -12$; c) bottom; 1) $\bar{x} = 0.45$; 2) $\bar{x} = 0.55$; 3) $\bar{x} = 0.65$; 4) $\bar{x} = 0.75$; 5) $\bar{x} = 0.8$; 6) $\Lambda = 0$].

The initial velocity profile ($\bar{x} = 0.25$) is in satisfactory agreement with the Pol'gauzen laminar profile. The separation profile differs very considerably from the Pol'gauzen separation profile ($\Lambda = -12$). The initial profile at the bottom of the cavity ($\bar{x} = 0.45$) is close to the separation profile at the back wall of the cavity. With an increase in $\bar{x}$ the profile first fills out and then becomes a separation profile again.

We also obtained the velocity distribution in a shallow cavity in the mixing zone and in the outer part of the wall jet (the flow region lying between the core of the stream and the boundary layer) in the turbulent mode of flow ($Re = 1.5 \cdot 10^4$). The velocity profile in the mixing zone agrees well with the universal jet velocity profile (1) [see Fig. 3: 4) $\bar{x} = 0.45$;

5) $\bar{x} = 0.5$; 6) $\bar{x} = 0.55$; 7) $\bar{x} = 0.65$], while the velocity distribution in the jet part of the wall jet (not presented in the article) retains the form of the velocity profile of that part of the jet in the mixing zone which turns into the cavity after hitting the back wall (below the line $y = 0$), i.e., exactly the same pattern as in a square cavity (Fig. 3 of [3]) is observed.

LITERATURE CITED

1. F. Pan and A. Acrivoc, "Steady flows in rectangular cavities," J. Fluid Mech., 28, Part 4 (1967).
2. S. N. Oka, "Flow field between two roughness elements in developed turbulent channel flow," in: Heat and Mass Transfer in Flows with Separated Regions, International Seminar, Herceg Novi, 1969, Pergamon Press, Oxford–New York (1972).
3. V. Ya. Bogatyrev, Yu. N. Dubnishchev, et al., "An experimental investigation of flow in a trench," Zh. Prikl. Mekh. Tekh. Fiz., No. 2 (1976).
4. A. S. Ginevskii, The Theory of Turbulent Jets and Wakes [in Russian], Mashinostroenie, Moscow (1969).
5. V. D. Zhak, V. A. Mukhin, and V. E. Nakoryakov, "Three-dimensional vortex structures in a cavity," Zh. Prikl. Mekh. Tekh. Fiz., No. 2 (1981).

FLOW OF A LIQUID FILM OVER THE INNER SURFACE OF A ROTATING CYLINDER

Yu. V. Martynov

UDC 532.516

1. The dimensionless equations of motion and continuity and the boundary conditions in a coordinate system y, z, φ (where $z = z^\circ$ is the axial coordinate, $\varphi = \varphi^\circ$, $y = R - r^\circ$, the origin is located on the joint between semiinfinite tubes, z°, r°, φ° is a cylindrical coordinate system) rotating about the axis of symmetry of a cylinder with the angular velocity of rotation of the upper semiinfinite tube have the form [1, 2]

$$\varepsilon\left(v_y\frac{\partial v_y}{\partial y}+v_z\frac{\partial v_y}{\partial z}+\frac{v_\theta^2}{\eta+y}\right)+2v_\theta=-\frac{\partial p}{\partial y}+E\left[\frac{\partial^2 v_y}{\partial y^2}+\frac{\partial^2 v_y}{\partial z^2}-\frac{1}{\eta+y}\frac{\partial v_y}{\partial y}-\frac{v_y}{(\eta+y)^2}\right], \tag{1.1}$$

$$\varepsilon\left(v_y\frac{\partial v_\theta}{\partial y}+v_z\frac{\partial v_\theta}{\partial z}+\frac{v_y v_\theta}{\eta+y}\right)+2v_y=E\left[\frac{\partial^2 v_\theta}{\partial y^2}+\frac{\partial^2 v_\theta}{\partial z^2}-\frac{1}{\eta+y}\frac{\partial v_\theta}{\partial y}-\frac{v_\theta}{(\eta+y)^2}\right],$$

$$\varepsilon\left(v_y\frac{\partial v_z}{\partial y}+v_z\frac{\partial v_z}{\partial z}\right)=-\frac{\partial p}{\partial z}+E\left(\frac{\partial^2 v_z}{\partial z^2}+\frac{\partial^2 v_z}{\partial y^2}-\frac{1}{\eta+y}\frac{\partial v_z}{\partial y}\right)+\frac{1}{\mathrm{Fr}},$$

$$\frac{\partial v_z}{\partial z}+\frac{\partial v_y}{\partial y}+\frac{v_y}{\eta+y}=0,\quad v_y=-v_r;$$

$$y=0,\ z<0,\ v_y=v_z=v_\theta=0, \tag{1.2}$$

$$z>0,\ v_y=v_z=0,\ v_\theta=\omega\eta;$$

$$y=h(z),\quad \left(\frac{\partial v_z}{\partial y}+\frac{\partial v_y}{\partial z}\right)(1+h_z^2)+4h_z\frac{\partial v_y}{\partial y}=0, \tag{1.3}$$

$$2E\frac{\partial v_y}{\partial y}(1-h_z^2)-Eh_z\left(\frac{\partial v_z}{\partial y}+\frac{\partial v_y}{\partial y}\right)-\frac{\alpha}{(\eta+y)^2}[h^2+(\eta+y)^2h_{zz}](1+h_z^2)=$$

$$=p(1+h_z^2),\quad v_y=h_z v_z,\quad \partial v_\theta/\partial y+v_\theta/(\eta+y)=0.$$

Boundary conditions as $z\to\pm\infty$ will be described below. The problem of Eqs. (1.1)-(1.3) is reduced to dimensionless form by replacement of the variables r, v, Ω, p by their

Moscow. Translated from Zhurnal Prikladnoi Mekhaniki i Tekhnicheskoi Fiziki, No. 3, pp. 75-82, May-June, 1984. Original article submitted May 4, 1983.

0021-8944/84/2503-0400$08.50

© 1984 Plenum Publishing Corporation